ELSEVIER

Carbohydrate Research 317 (1999) 223–228

CARBOHYDRATE RESEARCH

Note

The structure of cationic amylopectin as determined via mobility data compared to model calculations

Anders Larsson [a,*], Mikael Rasmusson [a], Hiroyuki Ohshima [b]

[a] *Department of Physical Chemistry, Göteborg University, Kemigården 3, SE-412 96 Göteborg, Sweden*
[b] *Faculty of Pharmaceutical Sciences, Science University of Tokyo, 12 Ichigaya Funagawara-machi, Shinjuku-ku, Tokyo 162, Japan*

Received 3 September 1998; accepted 25 February 1999

Abstract

The structure of cationic amylopectin has been investigated by means of the electrokinetic sonic amplitude (ESA) technique. The obtained mobility data have been evaluated with model calculations. Static light-scattering data are also presented and compared with model calculations. It was found that cationic amylopectin has a heterogenous structure. The mobility data could roughly be modelled with a soft sphere. The light-scattering data are an intermediate between a linear chain and a homogenously branched polymer.

Keywords: Electrokinetic sonic amplitude; Mobility; Static light scattering; Amylopectin

Cationic amylopectin and anionic nanosized silica particles are used in the paper industry to improve retention, dewatering and dry strength in the paper sheet [1]. The way in which they operate is not yet completely understood. During recent years a number of investigations have been performed to elucidate the dissolution of cationic amylopectin [2] and the interaction between the cationized amylopectin with salt and with nanosized silica particles [3–7]. It has become evident from these studies that an improved understanding of the three-dimensional structure of amylopectin is important to understand the flocculation behaviour. The tools used so far have been scattering techniques, which can give us some information about the structure of the amylopectin. The calculations of branched material are, however, formidable [8], and, therefore, it is reasonable to use simple models as in this paper. The calculations here consider how the mobility at different electrolyte concentrations is affected by various geometrical structures.

In Fig. 1, experimental data are compared with some chosen model calculations in a dimensionless Kratky plot form using static light-scattering data. The details of the experimental procedure and the exact form factors i.e., $P(q)$, will be discussed elsewhere [7]. It is required, however, to measure the intensity of scattered light of in this case vertically polarized incident light at a wavelength of 632.8 nm as a function of angle θ. The measurements

* Corresponding author. Tel.: +46-31-772-2748; fax: +46-31-167-194.
E-mail address: zoombie@phc.chalmers.se (A. Larsson)

0008-6215/99/$ - see front matter
PII: S0008-6215(99)00060-9

were plotted as Berry plots, as given by Eq. (1) [9],

$$\frac{Kc}{R_q} = \frac{(1 + A_2 M_w c)^2}{M_w P(q)} \quad (1)$$

where K is the optical constant, c is the concentration, R_q is the Rayleigh ratio at scattering vector q, A_2 is the second virial coefficient, M_w is the molecular weight and $P(q)$ is the form factor. The angle θ is related to the scattering vector q via

$$q = \frac{4\pi n_0}{\lambda_0} \sin(\theta/2) \quad (2)$$

where n_0 is the refractive index of the solvent and λ_0 is the wavelength of the incident light. At small q the reciprocal form factor is given by Eq. (3) [10],

$$\frac{1}{P(q)} = 1 + \frac{q^2 R_g^2}{3} \quad (3)$$

where R_g is the radius of gyration. In reality, the Berry plot is plotted as $(Kc/R_q)^{0.5}$ versus q^2. The form factor was obtained using Eq. (4),

$$P(q) = \frac{R(q)}{R(q=0)} \quad (4)$$

The dimensionless Kratky plot was obtained by plotting the dimensionless parameter $u = qR_g$ as the x-axis and at the y-axis $u^2P(q)$ is plotted.

The model calculations show that the term $P(q)u^2$ will be lower as the branching density increases [8]. It also demonstrates that polydispersity will increase the term $P(q)u^2$. There are model calculations of ABC type of polymers [8]. However, the obtained branching density is too low due to neglect of excluded volume of the individual branches. Polydispersity is also lacking in this calculation. The experimental light-scattering data indicate that the structure of cationic amylopectin is heterogenous and it cannot be understood by any simple scattering model. Therefore, it is useful to use methods other than scattering to obtain information about the structure of amylopectin.

The experimental method for determining dynamic mobility data is described elsewhere [4]. However, a measure of the ESA signal, i.e., the electrokinetic sonic amplitude, and a density term $\phi(\Delta\rho/\rho)$ are required to obtain the dynamic mobility according to Eq. (5),

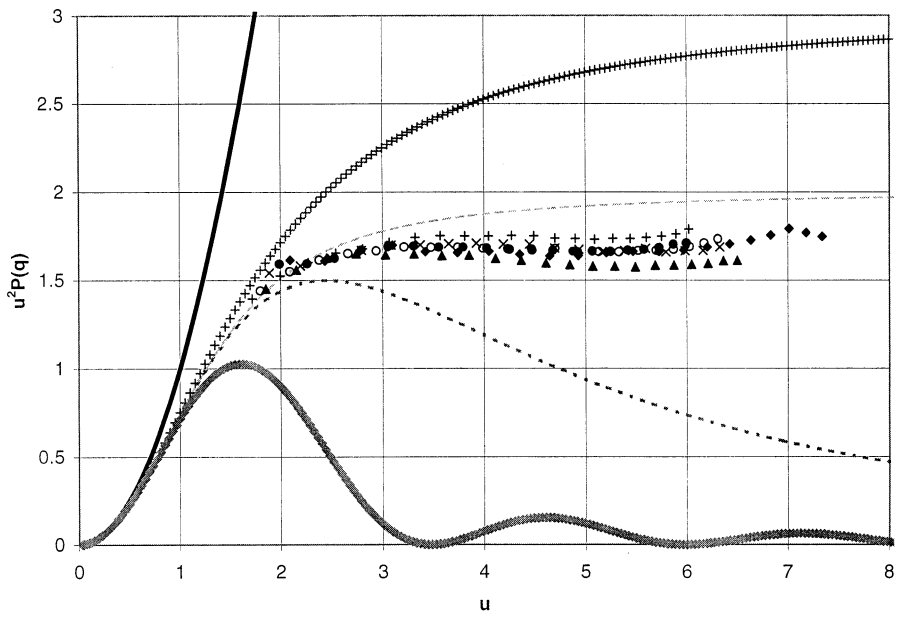

Fig. 1. A dimensionless Kratky plot showing how the internal structure of a cationic amylopectin (DS = 0.052) is affected by the addition of salt. The internal structure is within experimental error not affected by the presence of salt. For comparison, some theoretical model calculations shown. (Filled diamond) 0 mM, (filled triangle) 5 mM, (cross) 10 mM, (empty circle) 20 mM, (filled circle) 50 mM, and (dark plus sign) 100 mM added NaN_3; (shaded plus sign) linear chain polydisperse, (dark hyphenated line) homogenously branched, (thick filled line) thin rod, (thick shaded line) sphere, (shaded hyphenated line) linear chain monodisperse.

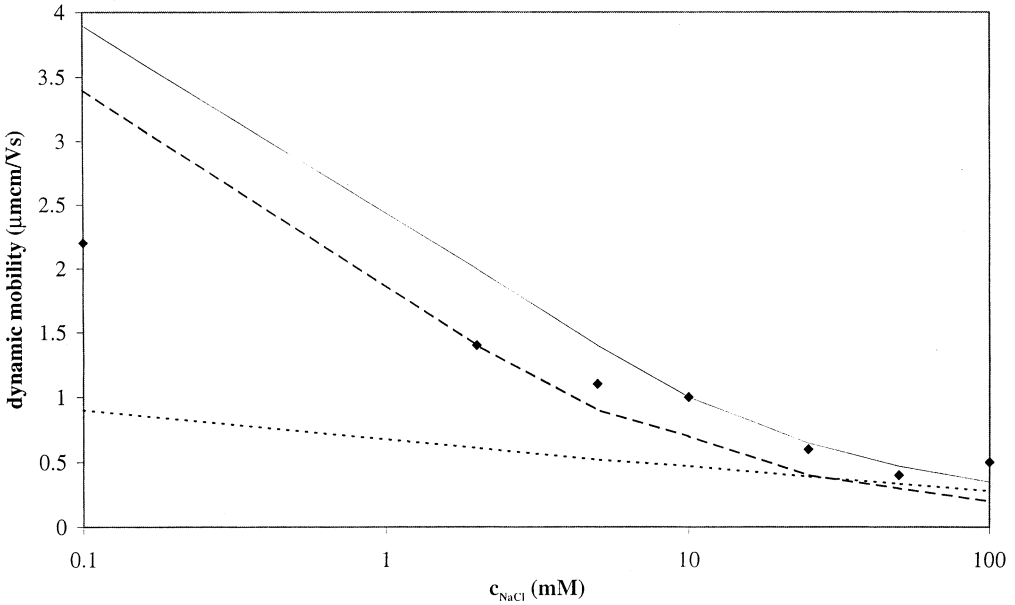

Fig. 2. The dynamic mobility of cationic amylopectin (DS = 0.052) as a function of salt concentration. Experimental points compared with a hard cylinder model and hard sphere radius (200 and 250 nm, respectively) are shown. (◆) Experimental; (- - -) cylinder; (– – –) 250 nm; (—) 200 nm.

$$\mathrm{ESA} = \phi\frac{\Delta\rho}{\rho}\mu_{\mathrm{d}} \tag{5}$$

where ϕ is the volume fraction of the hydrated polymer, $\Delta\rho$ is the density difference between the polymer and the solvent, ρ is the density of the solvent and μ_{d} is the dynamic mobility. The density measurements were repeated and the term $\phi(\Delta\rho/\rho)$ was now found to have a value of $(3.2 \pm 0.4) \times 10^{-4}$ independent of ionic strength (this value replaces Table 2 in [4]). The dynamic mobility was therefore recalculated from the ESA and density data and the result is shown in Fig. 2. The dynamic mobility and electrophoretic mobility probably coincide as long as the density difference between particles (polymers) and solvent is low, and then no inertia effect due to the applied electric field (≈ 1 MHz) is recognised, i.e., the phase angle is low. The phase angle was low for amylopectin and furthermore the dynamic and static electrophoretic mobility coincide (within experimental error) for DNA [11]. All model calculations are based on static electrophoretic mobility and will be compared with the obtained dynamic mobility.

The static electrophoretic mobility is calculated for a hard sphere and a hard cylinder and the result is displayed in Fig. 2. The mobility, μ, for the cylindrical model [12,13] was calculated from the following equations:

$$\sigma_0 = \varepsilon\varepsilon_0\kappa K1(\kappa a)\zeta\beta/K0(\kappa a) \tag{6}$$

and

$$\sigma_0 = ze/(2\pi ab) \tag{7}$$

and

$$\mu = 2\varepsilon\varepsilon_0\zeta/(3\eta) \tag{8}$$

where σ_0 is the charge density, ε is the dielectric constant of the solvent, ε_0 is the permitivity in vacuum, $K0$ and $K1$ are Bessel functions of zero and first order, respectively, κ is the Debye–Hückel parameter, ζ is the zetapotential, β is the correction factor which incorporates the non-linear charge–potential relationship, e is the elementary charge, z is the valency of the polyelectrolyte charges and $z = 1$ if b is taken as the distance between the charges, a is the cylinder radius and η is the viscosity of the solvent. The degree of substitution (DS) of the quaternary amine was 0.052 and the molecular weight of the amylopectin was 40×10^6 g/mol (which replace the former presented molecular weight). The molecular weight was obtained with static light scattering using the Berry plot procedure. The radius of the cylinder was found to be 2.5 Å and the distance between the charges was found to be 107.3 Å, as calculated from data for the glucose monomer. The charge density, σ_0, and

the electrophoretic mobility, μ, for the hard sphere [14,15] were calculated from the following equations:

$$\sigma_0 = \frac{\varepsilon\varepsilon_0\kappa kT}{ze}\left(2\sinh\left(\frac{ze\zeta}{2kT}\right) + \frac{4}{\kappa a}\tanh\left(\frac{ze\zeta}{4kT}\right)\right) \quad (9)$$

and

$$\mu = \frac{\varepsilon\varepsilon_0\zeta}{\eta} f(\kappa a) \quad (10)$$

$$f(\kappa a) = \frac{2}{3}\left[1 + \frac{1}{2[1 + (2.5/\kappa a\{1 + 2\exp(-\kappa a)\})]^3}\right] \quad (11)$$

where the abbreviations are identical to the cylinder model, except now it is the radius of the sphere, k is Boltzmann's constant and T is the absolute temperature.

The fixed parameters used in the cylinder and hard sphere model are: $z = 1$, $T = 298$ K, $k = 1.38 \times 10^{-23}$ J mol^{-1}, $e = 1.6 \times 10^{-19}$ C, $\varepsilon = 78.5$, $\varepsilon_0 = 8.85 \times 10^{-12}$ F m^{-1}, $\eta = 0.89 \times 10^{-3}$ Pa and $\beta = 1$. The hard sphere (with a radius of 200 nm) gives a reasonable mobility at intermediate electrolyte concentration but overestimates the mobility at low electrolyte concentration. The hard sphere (with a radius of 250 nm) gives a correct mobility at 2 mM NaCl but underestimates the mobility at high ionic strength. The number of surface charges is kept constant in these calculations so the surface charge density varies as the radius of the hard sphere changes. The cylinder model clearly underestimates the mobility, especially at low electrolyte concentration. It should also be emphasised that the mobility for hard cylinders and spheres tends to zero at high electrolyte concentrations. The data for the cationic amylopectin suggest that they obtain a finite plateau mobility at rather high electrolyte concentrations. This is also the case for soft-particle models, which we will focus on next.

The experimental mobility data shown in Fig. 2 were fitted with a porous sphere and with a soft sphere model to obtain a radius that could be compared to the radius of gyration obtained with static light scattering and the results are displayed in Fig. 3. The radius for the porous sphere [16,17], which fitted with the experimental mobility data, was calculated according to the following formulae,

$$\mu = \frac{\rho_{\text{fix}}}{\eta\lambda^2}[1 + g + hp] \quad (12)$$

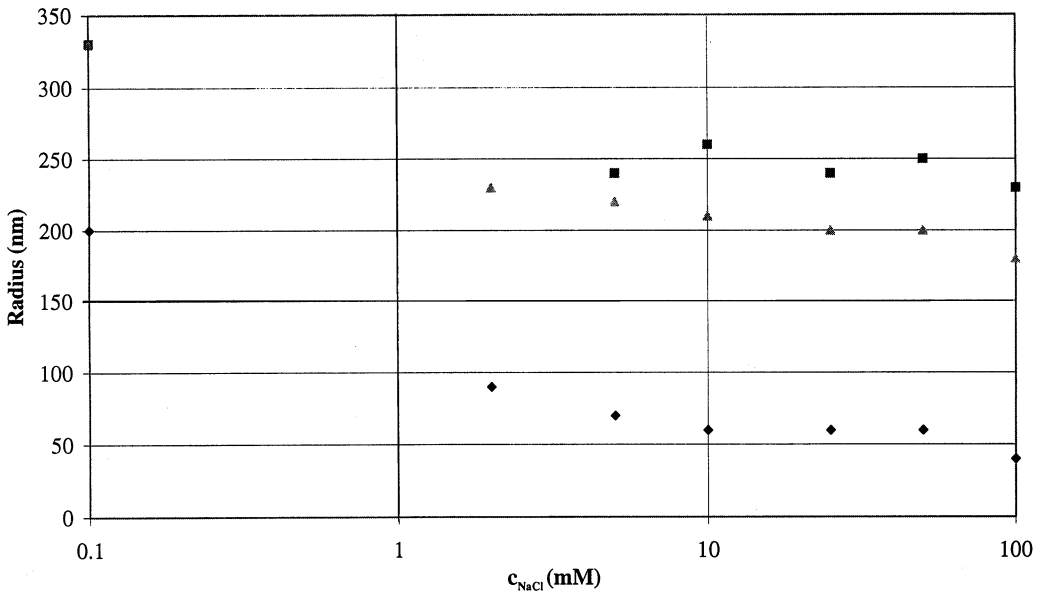

Fig. 3. The radius of gyration, denoted R_g, of cationic amylopectin as a function of electrolyte concentration. The radius of a porous sphere, denoted R_p, and the radius of a soft sphere, where the hardcore radius was set to 140 nm as a function of electrolyte concentration, are shown. (◆) R_p; (■) R_g; (▲) $a = 140$ nm.

$$g = \frac{1}{3}\left(\frac{\lambda}{\kappa}\right) \times {}^{2}\left\{1 + \exp(-2\kappa b) - \left(\frac{1-\exp(-2\kappa b)}{\kappa b}\right)\right\} \quad (13)$$

$$h = \frac{1}{3}\left(\frac{\lambda}{\kappa}\right)^{2} \frac{1+\left(\frac{1}{\kappa b}\right)}{\left[\left(\frac{\lambda}{\kappa}\right)^{2}-1\right]} \quad (14)$$

$$p = \frac{\lambda}{\kappa}\frac{1+\exp(-2\kappa b) - \frac{1-\exp(-2\kappa b)}{\kappa b}}{\left(\frac{1+\exp(-2\lambda b)}{1-\exp(-2\lambda b)} - \frac{1}{\lambda b}\right)} - [1-\exp(-2\kappa b)] \quad (15)$$

where

$$\rho_{\mathrm{fix}} = \mathrm{DS}ev \quad (16)$$

$$v = \frac{3N}{4\pi b^{3}} \quad (17)$$

$$n_{\mathrm{salt}} = jN_{\mathrm{a}} \quad (18)$$

$$\sigma = \left(\frac{vfb^{2}}{\eta}\right)^{1/2} \quad (19)$$

$$\lambda = \frac{\sigma}{b} \quad (20)$$

$$f = 6\pi\eta a_{1} \quad (21)$$

where DS is the degree of substitution of charges, i.e., DS = 0.052 in this case, e is the elementary charge, N is the number of polymer beads in the porous sphere ($N = 247 \times 10^{3}$) with radius b ($b = 2.5$ Å), j is the ionic strength (in mol/m^{3}), N_{a} is Avogadro's number, σ is the Debye shielding parameter, η is the viscosity of the solvent and a_{1} is the radius of one polymer bead, z is the valency of the charged groups in the polymer and κ is the Debye–Hückel screening parameter.

Eqs. (22)–(25) are used to calculate the radius of the hard core and the extension of the polymer layer by fitting the experimental mobility data for a soft sphere [17,18] as follows:

$$\mu = \frac{2}{3}\frac{\varepsilon\varepsilon_{0}}{\eta}\frac{\frac{\psi_{0}}{\kappa_{m}} + \frac{\psi_{\mathrm{DON}}}{\lambda}}{\frac{1}{\kappa_{\mathrm{m}}} + \frac{1}{\lambda}} \times \left[1 + \frac{1}{2\left(1+\frac{d}{a}\right)^{3}}\right] + \frac{\rho_{\mathrm{fix}}}{\eta\lambda^{2}} \quad (22)$$

$$\kappa_{\mathrm{m}} = \kappa\left[1 + \left(\frac{\rho_{\mathrm{fix}}}{2zen_{\mathrm{salt}}}\right)^{2}\right]^{1/4} \quad (23)$$

$$\psi_{\mathrm{DON}} = \frac{kT}{ze}\ln\left[\frac{\rho_{\mathrm{fix}}}{2zen_{\mathrm{salt}}} + \left\{1 + \left(\frac{\rho_{\mathrm{fix}}}{2zen_{\mathrm{salt}}}\right)^{2}\right\}^{1/2}\right] \quad (24)$$

$$\psi_{0} = \psi_{\mathrm{DON}} + \frac{2n_{\mathrm{salt}}kT}{\rho_{\mathrm{fix}}}\left[1 - \left\{\left(\frac{\rho_{\mathrm{fix}}}{2zen_{\mathrm{salt}}}\right)^{2} + 1\right\}^{1/2}\right] \quad (25)$$

where the abbreviations used are the same as before with the following exceptions: ψ_{DON} is the Donnan potential in the polymer layer, ψ_{0} is the potential at the surface of the polymer layer, κ_{m} is the Debye–Hückel parameter in the polymer layer, a is the radius of the particle core and d is the extension of the polymer shell.

All parameters were fixed except the ones connected to the radii of the porous and soft spheres. The fixed parameters are: $z = 1$, $T = 298$ K, $N_{\mathrm{A}} = 6.022 \times 10^{23}$ mol^{-1}, $k = 1.38 \times 10^{-23}$ J mol^{-1}, $e = 1.6 \times 10^{-19}$ C, $\varepsilon = 78.5$, $\varepsilon_{0} = 8.85 \times 10^{-12}$ F m^{-1} and $\eta = 0.89 \times 10^{-3}$ Pa. Note the good agreement between the radius of gyration and the soft sphere model when the hard core was set to 140 nm. However, it must be pointed out that the fit is rather insensitive to the size of the hard core of the soft sphere, probably for the same reasons that the mobility is rather insensitive of the hard sphere radius with a constant charge density. The radius of the soft layer is more or less the same as the porous sphere radius. The soft models has a finite mobility at high electrolyte concentrations because a term $\rho_{\mathrm{fix}}/(\eta\lambda^{2})$ remains that is insensitive to electrolyte concentration. This plateau value can also be seen for cationic amylopectin in Fig. 2.

Scattering, as well as electrokinetic data, shows that cationic amylopectin is an intermediate structure between a cylinder (rod) and a compact sphere. Further, more detailed modelling suggests that the structure is heterogenous. Modelling of scattering data suggests the structure to be somewhere between a lin-

ear chain and a homogenously branched polymer. Modelling of electrokinetic data suggests that the structure can be modelled roughly as a soft sphere.

Acknowledgements

Professor Walther Burchard is gratefully acknowledged for useful suggestions concerning modelling of light-scattering data. Financial support was obtained from Eka Chemicals AB.

References

[1] K. Andersson, E. Lindgren, *Nord. Pulp Pap. Res. J.*, 1 (1996) 15.
[2] A. Larsson, S. Wall, *Starch/Stärke*, 49 (1997) 396.
[3] A. Larrson, S. Wall, *Colloid. Surf. A: Physicochem. Eng. Asp.*, 139 (1998) 259.
[4] A. Larsson, M. Rasmusson, *Carbohydr. Res.*, 304 (1997) 315.
[5] A. Dahlberg, A. Larsson, B. Åkerman, S. Wall, *Colloid Polym. Sci.*, 277 (1999) 428.
[6] A. Dahlberg, A. Larsson, B. Åkerman, S. Wall, *Colloid Polym. Sci.*, 277 (1998) 436.
[7] A. Larsson, *Colloid. Surf. B: Biointerfaces*, 12 (1998) 23.
[8] W. Burchard, *Adv. Polym. Sci.*, 48 (1983) 1.
[9] G.C. Berry, *J. Chem. Phys.*, 44 (1966) 4550.
[10] A. Guinier, G. Fournet, *Small-Angle Scattering of X-rays*, Wiley, London, 1955, p 126.
[11] M. Rasmusson, B. Åkerman, *Langmuir*, in press.
[12] D. Stigter, *J. Colloid Interface Sci.*, 53 (1975) 296.
[13] D. Stigter, *J. Phys. Chem.*, 82 (1978) 1417.
[14] A.L. Loeb, J.Th.G. Overbeek, P.H. Wiersema, *The Electrical Double Layer around a Spherical Colloid Particle*, MIT Press, Cambridge, MA, 1961, p 37.
[15] H. Ohshima, *J. Colloid Interface Sci.*, 168 (1994) 269.
[16] J.J. Hermans, H. Fujita, *Koninkl. Ned. Akad. Wetenschap. Proc., Ser. B*, 58 (1955) 182.
[17] H. Ohshima, *J. Colloid Interface Sci.*, 163 (1994) 474.
[18] H. Ohshima, *Colloid. Surf. A: Physicochem. Eng. Asp.*, 103 (1995) 249.